Webb, A.A.G., Müller, T., Zuo, J., Haproff, P.J., and Ramírez-Salazar, A., 2020, A non–plate tectonic model for the Eoarchean Isua supracrustal belt: Lithosphere, https://doi.org/10.1130/L1130.1.

Data Repository

Figure DR1. Schematic geologic map of the Isua supracrustal belt (modified from Figure 1) showing the distribution of shear-sense indicators observed during our field work and the locations of photographs presented in Figure DR2. The inset map displays a portion of the geologic map containing km-scale bulls-eye map patterns manifested by 3.7 Ga chert/BIF and low Al_2O_3/TiO_2 basalts; bulls-eye map patterns are consistent with sheath folding.

Figure DR2. Photographs of key geological relationships at the Isua supracrustal belt. Locations are marked on Figure DR1's map.

Figure DR1.

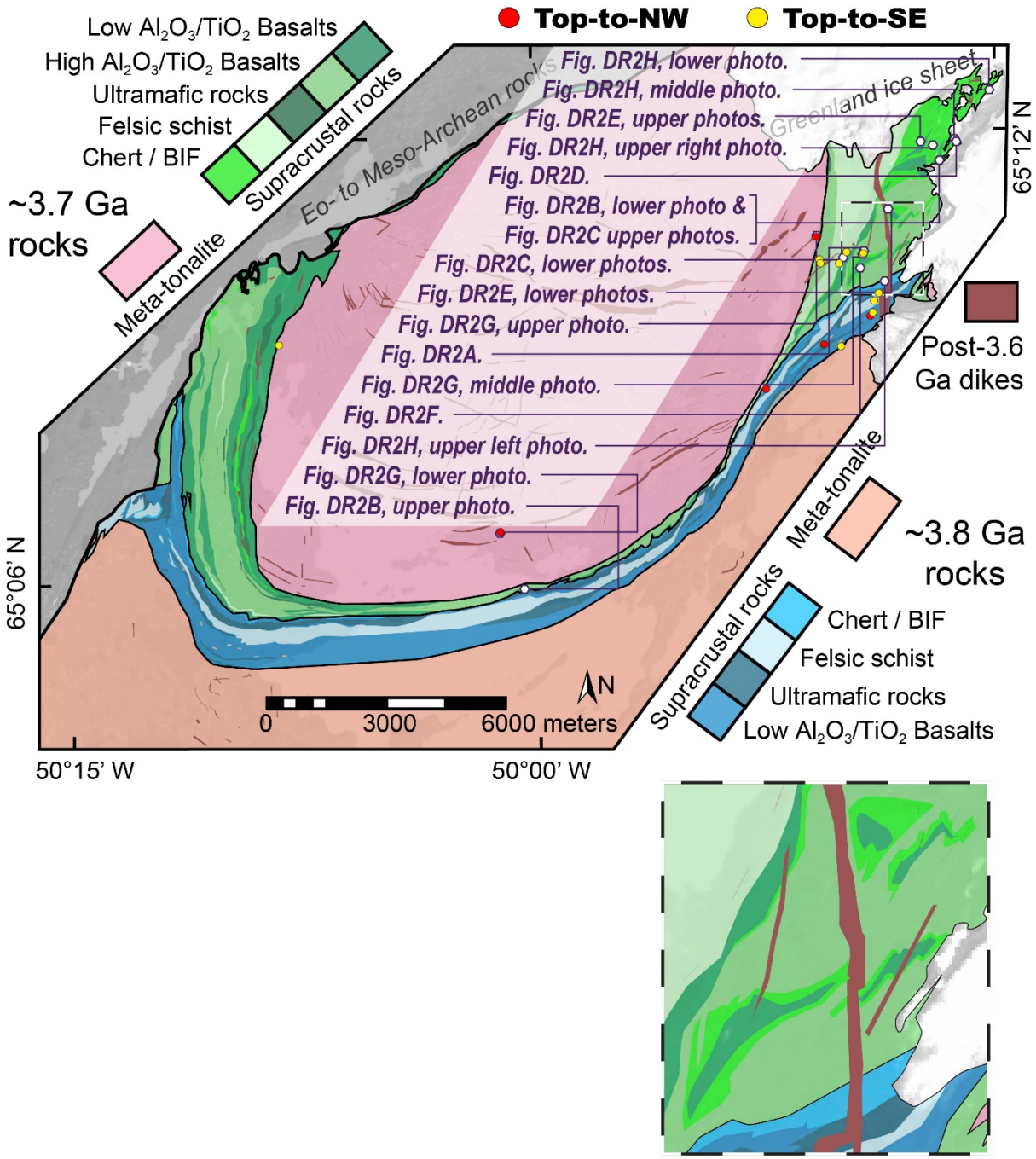
Top-to-NW
Top-to-SE
Low Al_2O_3/TiO_2 Basalts
High Al_2O_3/TiO_2 Basalts
Ultramafic rocks
Felsic schist
Chert / BIF
Supracrustal rocks
~3.7 Ga rocks
Meta-tonalite
Eo- to Meso-Archean rocks
Greenland ice sheet
Fig. DR2H, lower photo.
Fig. DR2H, middle photo.
Fig. DR2E, upper photos.
Fig. DR2H, upper right photo.
Fig. DR2D.
Fig. DR2B, lower photo &
Fig. DR2C upper photos.
Fig. DR2C, lower photos.
Fig. DR2E, lower photos.
Fig. DR2G, upper photo.
Fig. DR2A.
Fig. DR2G, middle photo.
Fig. DR2F.
Fig. DR2H, upper left photo.
Fig. DR2G, lower photo.
Fig. DR2B, upper photo.
65°12' N
65°06' N
50°15' W
50°00' W
0
3000
6000 meters
N
Post-3.6 Ga dikes
Meta-tonalite
~3.8 Ga rocks
Supracrustal rocks
Chert / BIF
Felsic schist
Ultramafic rocks
Low Al_2O_3/TiO_2 Basalts

Figure DR2.

Figure DR2A. As in Figure 4A, this site shows that metamorphosed and strained pillow lavas do not preserve significantly lower strain versus the bulk of the belt, because the same penetrative lineation pervades the entire belt. The upper view looks down the lineation direction, with dark ellipses marking the metamorphosed rims of pillows (six-inch red-tinted ruler for scale). The lower view looks perpendicular to the lineation and parallel to the foliation, revealing the penetrative strain preserved here (compass for scale).

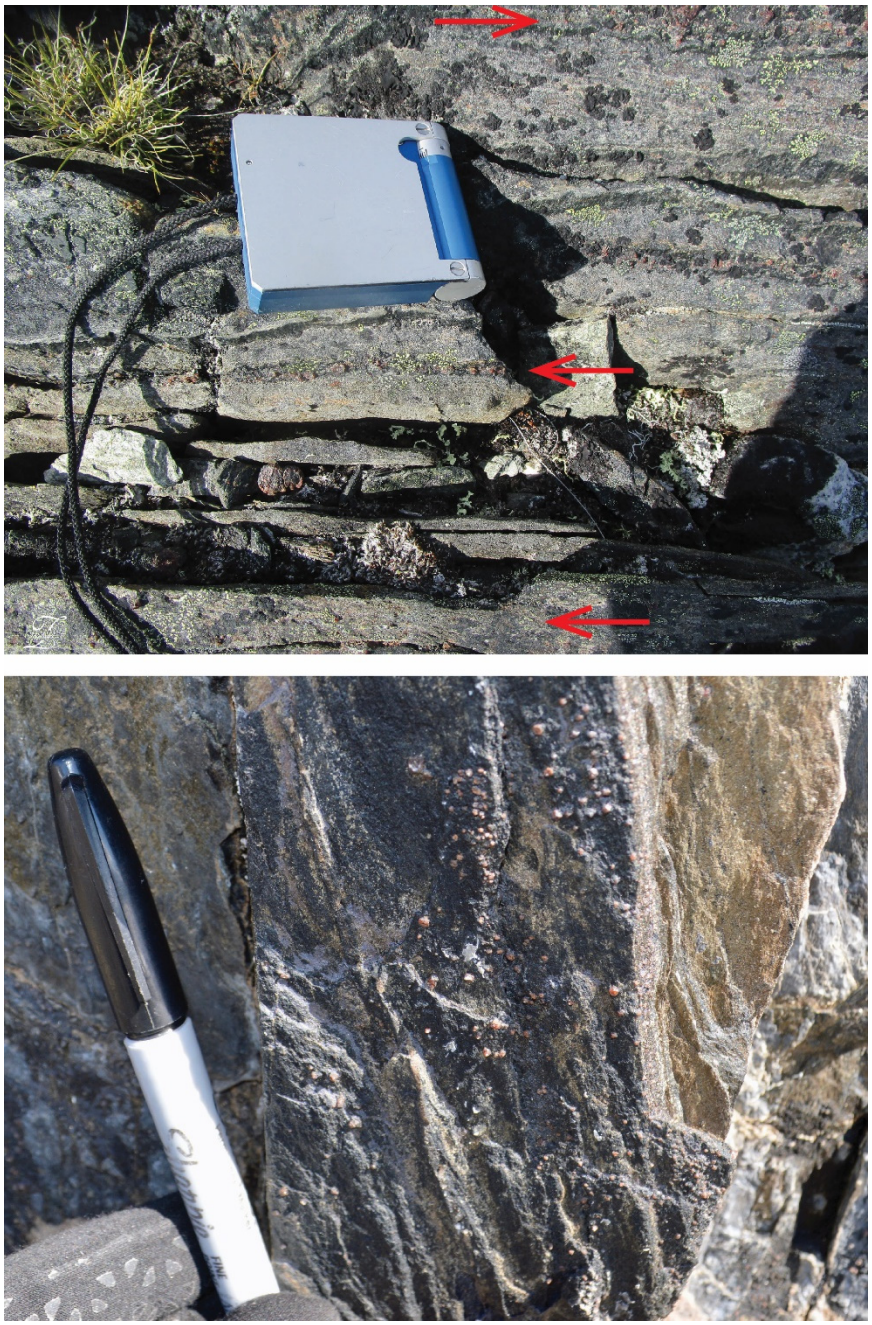

Figure DR2B. Garnet-bearing mafic schists occur along the entire Isua supracrustal belt, such that amphibolite-facies prograde conditions were experienced by the entire belt. The upper photograph is from the southern portions of the Isua supracrustal belt (layers containing red garnets are highlighted by red arrows). The lower photograph is from the northeastern Isua supracrustal belt.

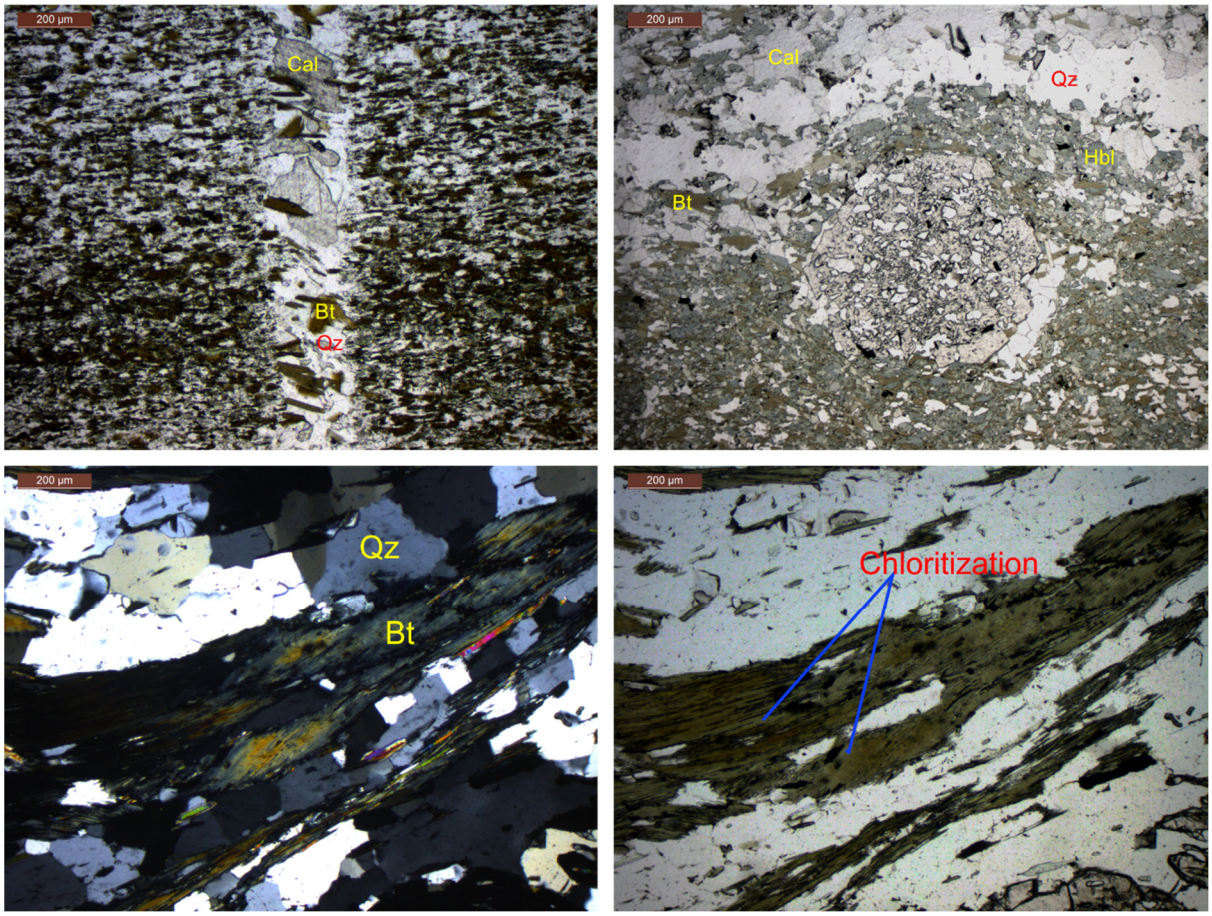

Figure DR2C. Photomicrographs showing key features of metamorphism in the northeasternmost portion of the Isua supracrustal belt. Upper-left photo shows quartz (Qz)-calcite (Cal) veins cross-cutting the main foliation in a sample from the northernmost part of the belt. Upper-right picture shows euhedral inclusion-rich garnet (inclusions mainly of calcite and quartz; center of the photo) in the northeasternmost part of the belt, suggesting a pervasive amphibolite facies metamorphism. Lower photos display partially chloritized biotite showing that the chlorite mimics the foliation and therefore could be misinterpreted as prograde chlorite.

Figure DR2D. Quartz-calcite veins showing pervasive metasomatic alteration in the northeastern portion of the Isua supracrustal belt.

Figure DR2E. Lithologic contacts in the Isua supracrustal belt show penetrative deformation consistent with fabrics seen across the rest of the belt. The upper photos show a metabasalt – chert/banded iron formation contact featuring cm-scale interlayering of these units along the contact. The lower photos show a different contact with similar lithologies, and similarly coherent, penetrative deformation fabrics (i.e., foliation and lineation) developed across the contact.

Figure DR2F. Key fault, fold, and stretching fabric patterns occur at the dark hill in upper photograph (center foreground). The middle photos show two faults. At left, the classic example from Komiya et al. (1999, their Figure 2) is shown in a somewhat larger view, including additional complex folding to the lower right. At right, termination of chert-pebble meta-conglomerate layers reveals another fault surface. The lower photos reveal that although the meta-conglomerate appears to have largely escaped deformation when viewed parallel to the lineation (left photo), the lineation-perpendicular view (afforded by prior dynamite blasting, right photo) reveals that these rocks do not preserve significantly lower strain versus the bulk of the belt. As discussed in the main text, we interpret the deformation observed here within the context of sheath and curtain folds which include relatively minor tearing of layers.

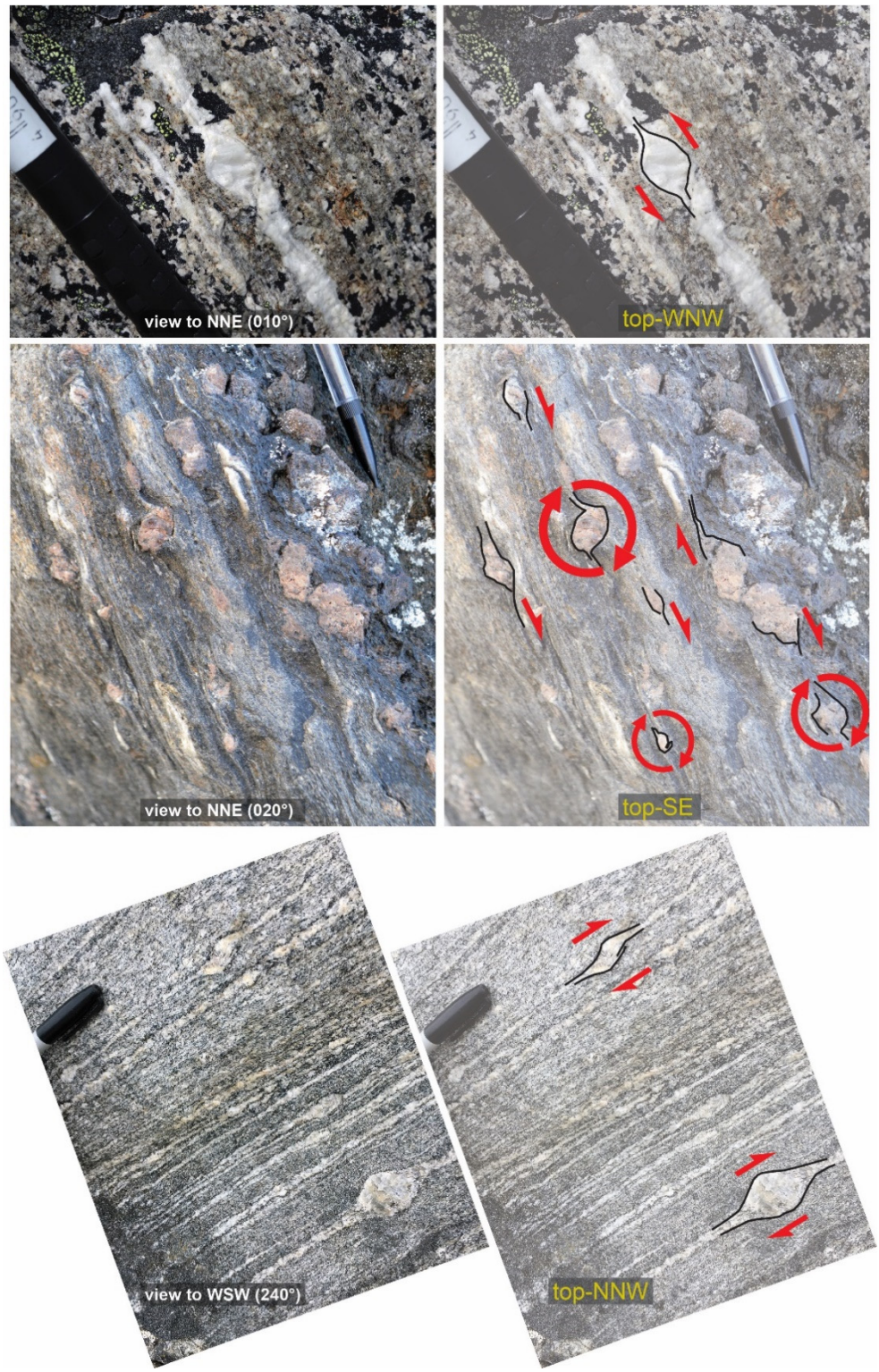

Figure DR2G. Examples of top-NW and top-SE shear sense indicators observed along the Isua supracrustal belt. The upper and lower photographs show top-NW sigma structures developed in TTG gneiss; the middle photograph shows top-SE sigma and delta structures developed in garnet schist.

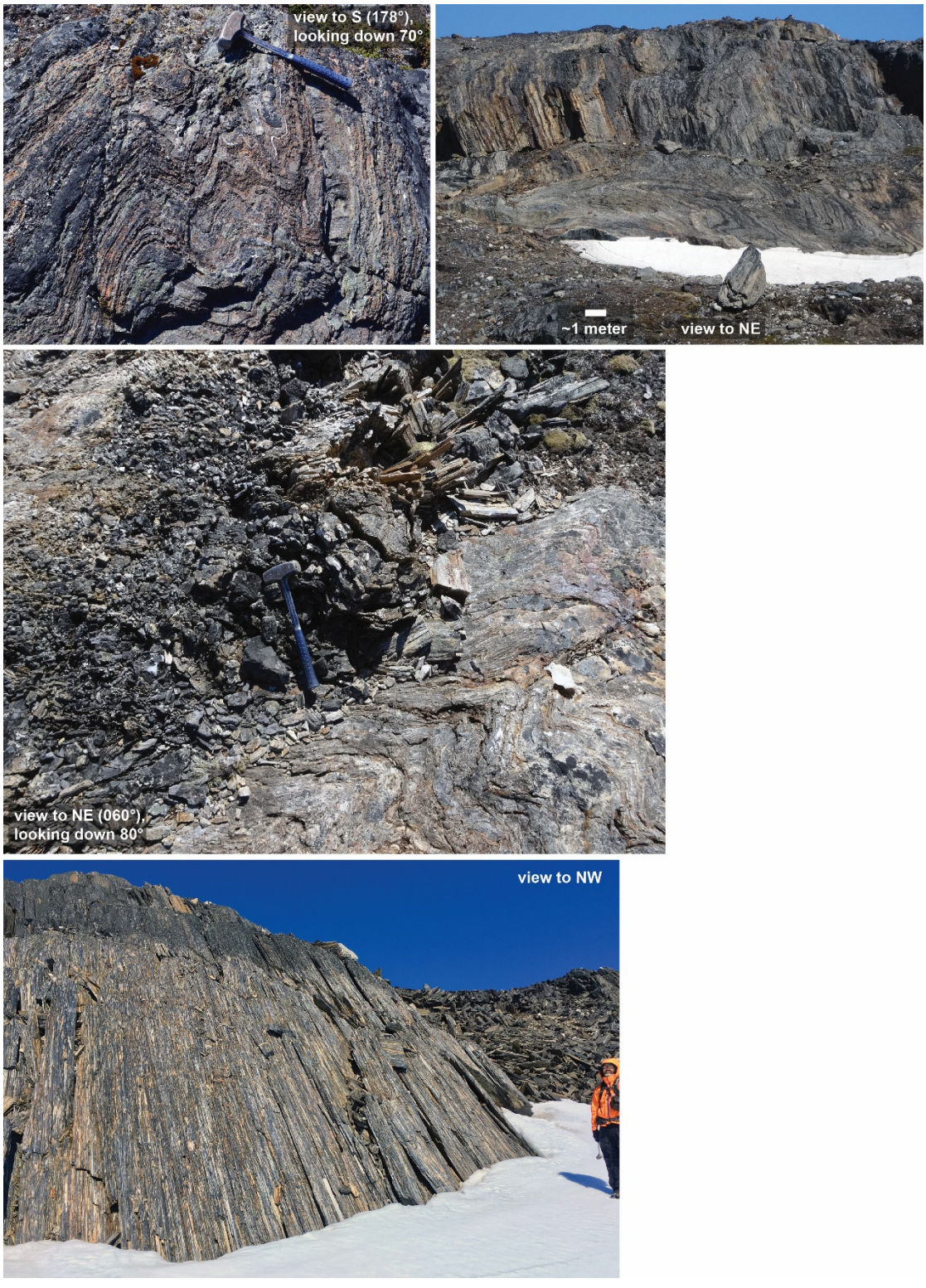

Figure DR2H. The upper photos show examples of dm- to m-scale curtain folds in the Isua supracrustal belt. The middle photo shows how such folds commonly coincide with rodded cleavage indicating strong prolate stretching (shown particularly clearly by the fallen rodded blocks to the upper right). Similar patterns occur at the Pilbara greenstone belt (e.g., Collins et al., 1998). The lower photo shows dramatic development of rodded (or 'pencil') cleavage.

DATA REPOSITORY REFERENCES CITED

Collins, W. J., Van Kranendonk, M. J., and Teyssier, C., 1998, Partial convective overturn of Archaean crust in the east Pilbara Craton, Western Australia: driving mechanisms and tectonic implications: Journal of Structural Geology, v. 20, no. 9-10, p. 1405-1424.

Komiya, T., Maruyama, S., Masuda, T., Nohda, S., Hayashi, M., and Okamoto, K., 1999, Plate tectonics at 3.8-3.7 Ga: Field evidence from the Isua Accretionary Complex, southern West Greenland: Journal of Geology, v. 107, no. 5, p. 515-554.